Synthesis of Linear and Planar Arrays With Minimum Element Selection

R. C. Nongpiur, *Member, IEEE,* and D. J. Shpak, *Senior Member, IEEE*

***Abstract*—A new method for the synthesis of linear and planar arrays having prescribed beamwidth and sidelobe levels and a minimum number of elements is proposed. In the method, the number of elements in an array is minimized while constraining the amplitude-response error in the mainlobe region, the attenuation in the sidelobe region, and the array dimensions. An iterative constrained optimization method is used where the amplitude-response error is linearly approximated at each iteration while concurrently minimizing a re-weighted L_1 norm of the array coefficients. To ensure robustness of the array, we constrain a sensitivity parameter, namely, the white noise gain, to be above a prescribed level. Furthermore, the method also provides the additional flexibility of controlling the array dimensions, symmetry properties, and element positions of the array. Two variants have been developed: In the first variant, both the array coefficients and the positions of the elements are optimized; in the second variant only the array coefficients are optimized while the elements are fixed at predefined positions. Experimental comparisons with several state-of-the-art competing methods show that the proposed method provides greater flexibility of controlling the robustness, beampattern response error, array dimensions, and element positions while at the same time the number of elements is less than or equal to that of the competing methods.**

***Index Terms*—array synthesis, beampattern, sparse arrays, optimization**

I. Introduction

Reducing the number of elements in an array offers several advantages such as lower cost, weight, power consumption, and heat dissipation. In digital beamforming arrays, this advantage is reflected as a reduction in computational complexity. The problem of reducing the number of elements in an array is a highly nonlinear problem and finding the global optimum consistently is very difficult, although good sub-optimal solutions can often be obtained.

Over the past five decades, many techniques for the design of arrays with a reduced number of elements have been proposed [1]-[11]. More recently, new techniques such as matrix pencil methods [12]-[14], constrained optimization methods [15]-[17], compressive sensing methods [18]-[21], and analytical methods [22]-[23] have been successfully applied in designing arrays with a reduced number of elements. The matrix pencil methods yield arrays that have elements in arbitrary positions and are useful when the elements are not constrained to predefined positions. On the other hand, the constrained optimization methods in [15]-[18] yield arrays with a minimum number of elements from a predefined set, and are appropriate when the elements are constrained to predefined positions such as with a reconfigurable array [24]. For clarity, it should be pointed out that in multiple-input multiple-output (MIMO) radar [25]-[28], the method for realizing the transmit beampattern is different from the method described in this paper. While the desired transmit beampattern in MIMO radar is obtained by modifying the covariance matrix of the transmitted signal, the method in this paper uses the beamforming approach where the array coefficients are modified.

In this paper, we propose a new array design method that minimizes the number of elements in an array with either predefined or arbitrary positions. In the method, the number of elements is minimized while maintaining the amplitude-response error in the mainlobe region and the attenuation in the sidelobe region within prescribed levels. The problem is solved as an iterative constrained optimization problem where the amplitude-response error is linearly approximated at each iteration while minimizing a re-weighted L_1 norm of the array coefficients. To ensure robustness of the array, we constrain a sensitivity parameter, namely, the white noise gain (WNG), to be above a prescribed level. The use of the WNG constraint is not new and has been used in earlier arrays designs to ensure robustness in beamformers [29]-[31]. Furthermore, the method also provides the additional flexibility of controlling the array dimensions, symmetry properties, and element positions of the array. Two variants have been developed. In the first variant, both the array coefficients and the positions of the elements are optimized while in the second variant only the array coefficients are optimized and the elements are fixed at predefined positions. Experimental comparisons with state-of-the-art competing methods show that the proposed method provides greater flexibility in controlling the robustness, beampattern response error, array dimensions, and element positions while at the same time the number of elements is less than or equal to that of the competing methods. In addition, we extended the one-dimensional nonuniform variable sampling approach, developed in [32] for the design of digital filters, to evaluate across the two-dimensional direction cosines in planar arrays, which considerably reduces the computational effort required.

The paper is organized as follows. In Section II, we describe the model of an array and the formulation for the beampattern response. Then in Section III we frame the design as a constrained optimization problem and in Section IV we carry out experimental comparisons with existing methods. Conclusions

R. C. Nongpiur and D. J. Shpak are with the Department of Electrical and Computer Engineering, University of Victoria, Victoria, BC, Canada V8W 3P6 e-mail: rnongpiu@ece.uvic.ca; dshpak@ece.uvic.ca

Manuscript submitted January 2014.

are drawn in Section V.

II. Beampattern of the Array

If M and N are the number of elements along the x and y directions, respectively, and $d_x(m,n)$ and $d_y(m,n)$ are the positions of each element along the x and y directions, the beampattern of the array can be expressed as

$$B(u_x,u_y)=\sum_{n=0}^{N-1}\sum_{m=0}^{M-1}a_{m,n}e^{j2\pi\xi(m,n)} \tag{1}$$

where

$$\begin{aligned}\xi(m,n) &= \frac{d_x(m,n)u_x+d_y(m,n)u_y}{\lambda} &(2)\\ a_{m,n} &= a_{m,n}^{(r)}+ja_{m,n}^{(i)} &(3)\end{aligned}$$

$a_{m,n}$ is the complex coefficient of the element, λ is the wavelength of the signal that impinges the array at an azimuth of ϕ and an elevation of θ, and u_x and u_y are the direction cosines given by

$$\begin{aligned}u_x &= \sin\theta\cos\phi\\ u_y &= \sin\theta\sin\phi &(4)\end{aligned}$$

For a linear array, $N=1$ and $\phi=0$ and (1) reduces to

$$\begin{aligned}B(u_x) &= \sum_{m=0}^{M-1}a_m e^{j2\pi d_x(m)u_x/\lambda} &(5)\\ a_m &= a_m^{(r)}+ja_m^{(i)} &(6)\\ u_x &= \sin\theta &(7)\end{aligned}$$

In matrix form, (1) can be expressed as

$$B(\mathbf{a},\mathbf{d},u_x,u_y)=\mathbf{g}(\mathbf{d},u_x,u_y)^T\mathbf{a} \tag{8}$$

where

$$\begin{aligned}\mathbf{a}^T &= \left[\bar{\mathbf{a}}_0^T\ \bar{\mathbf{a}}_1^T\cdots\ \bar{\mathbf{a}}_{N-1}^T\right]\\ \mathbf{d}^T &= \left[\mathbf{d}_x^T\ \mathbf{d}_y^T\right]\\ \mathbf{d}_x &= [d_x(0,0)\cdots d_x(M-1,N-1)]^T\\ \mathbf{d}_y &= [d_y(0,0)\cdots d_y(M-1,N-1)]^T\\ \mathbf{g}(\mathbf{d},u_x,u_y)^T &= \left[\mathbf{g}_0(\mathbf{d},u_x,u_y)^T\cdots\mathbf{g}_{N-1}(\mathbf{d},u_x,u_y)^T\right]\\ \bar{\mathbf{a}}_n &= \left[a_{0,n}^{(r)}\ a_{0,n}^{(i)}\cdots a_{M-1,n}^{(r)}\ a_{M-1,n}^{(i)}\right]^T\\ \mathbf{g}_n(\mathbf{d},u_x,u_y) &= [g_{0,n}(\mathbf{d},u_x,u_y)\cdots\\ &\qquad g_{M-1,n}(\mathbf{d},u_x,u_y)]^T\\ g_{m,n}(\mathbf{d},u_x,u_y) &= \exp\left[j\frac{2\pi}{\lambda}(d_x(m,n)u_x+\right.\\ &\qquad \left.d_y(m,n)u_y)\right]\end{aligned} \tag{9}$$

If $u_x^{(d)}$ and $u_y^{(d)}$ are the direction cosines corresponding to the desired look direction, the WNG of the array is given by [30]

$$G_w=\frac{|\mathbf{g}(\mathbf{d},u_x^{(d)},u_y^{(d)})^T\mathbf{a}|^2}{\mathbf{a}^T\mathbf{a}} \tag{10}$$

A. The Mainlobe Error

If $B_d(u_x,u_y)$ is the desired response of the beampattern, the squared amplitude-response error between the beamformer response and the desired beampattern in the mainlobe region when both the element coefficients, $\mathbf{a}$, and positions, $\mathbf{d}$, are optimized is given by

$$e_m(\mathbf{z},u_x,u_y)=|B(\mathbf{a},\mathbf{d},u_x,u_y)|^2-|B_d(u_x,u_y)|^2 \tag{11}$$

where

$$\mathbf{z}^T=[\mathbf{a}^T\ \mathbf{d}^T] \tag{12}$$

As in [33], we can incorporate the L_p norm of the squared mainlobe amplitude-response error, $E_p^{(\mathrm{ML})}$, in an iterative optimization problem by approximating $E_p^{(\mathrm{ML})}$ for the kth iteration by a linear approximation given by

$$\mathbf{E}_p^{(\mathrm{ML})}(k) \approx \|\mathbf{C}_k\boldsymbol{\delta}_z+\mathbf{f}_k\|_p \tag{13}$$

where

$$\begin{aligned}\mathbf{C}_k &= \begin{bmatrix}\kappa_m\nabla e_m(\mathbf{z}_k,u_x^{(1)},u_y^{(1)})^T\\ \vdots\\ \kappa_m\nabla e_m(\mathbf{z}_k,u_x^{(K_m)},u_y^{(K_m)})^T\end{bmatrix} &(14)\\ \mathbf{f}_k &= [f_1\ f_2\ \cdots\ f_{K_m}]^T &(15)\\ f_i &= \kappa_m e_m(\mathbf{z}_k,u_x^{(i)},u_y^{(i)}),\quad \{u_x^{(i)},u_y^{(i)}\}\in\Psi_{\mathrm{ML}} &(16)\end{aligned}$$

$\mathbf{z}_k$ is the value of $\mathbf{z}$ in the kth iteration, $\boldsymbol{\delta}_z$ is the update to $\mathbf{z}_k$, Ψ_{ML} is the set of direction cosines in the mainlobe region, κ_m is a discretization constant, and K_m is the total number of sample points. The right-hand side of (13) is the L_p norm of an affine function of $\boldsymbol{\delta}_z$ and, therefore, it is convex with respect to $\boldsymbol{\delta}_z$ [34]. Note also that the linear approximation in (13) is more accurate for smaller values of $\|\boldsymbol{\delta}_z\|_2$ and, therefore, $\|\boldsymbol{\delta}_z\|_2$ is constrained to be small.

If the positions of the elements are fixed then $\mathbf{d}$ is a constant and only the coefficients of the elements are optimized. Consequently, the mainlobe error is defined as

$$\hat{e}_m(\mathbf{a},u_x,u_y)=|B(\mathbf{a},\mathbf{d},u_x,u_y)|^2-|B_d(u_x,u_y)|^2 \tag{17}$$

and the linear approximation for the kth iteration is given by

$$\hat{\mathbf{E}}_p^{(\mathrm{ML})}(k) \approx \|\hat{\mathbf{C}}_k\boldsymbol{\delta}_a+\hat{\mathbf{f}}_k\|_p \tag{18}$$

where $\hat{\mathbf{C}}_k$ and $\hat{\mathbf{f}}_k$ are equivalent to (14) and (15), respectively, when $e_m(\mathbf{z},u_x,u_y)$ is replaced by $\hat{e}_m(\mathbf{a},u_x,u_y)$.

B. The Sidelobe Error

For the sidelobe region, $B_d(u_x,u_y)$ is set to zero and therefore the sidelobe error corresponds to the beamformer response, given by

$$e_s(\mathbf{z},u_x,u_y)=B(\mathbf{a},\mathbf{d},u_x,u_y) \tag{19}$$

As in the previous subsection, the L_p norm of the error in the sidelobe region for the kth iteration can be expressed as

$$\mathbf{E}_p^{(\mathrm{SL})}(k) \approx \|\mathbf{D}_k\boldsymbol{\delta}_z+\mathbf{g}_k\|_p \tag{20}$$

where $\mathbf{D}_k$ and $\mathbf{g}_k$ are equivalent to (14) and (15), respectively, when $e_m(\mathbf{z},u_x,u_y)$ is replaced by $e_s(\mathbf{z},u_x,u_y)$ and Ψ_{ML} by

Ψ_{SL}, where Ψ_{SL} is the set of direction cosines in the sidelobe region.

If the element positions are not optimized, $\mathbf{d}$ is a constant and, as a consequence, the sidelobe error is defined as

$$\hat{e}_s(\mathbf{a}, u_x, u_y) = B(\mathbf{a}, \mathbf{d}, u_x, u_y) \tag{21}$$

The L_p-norm of (21) can be expressed as a convex function given by

$$\mathcal{E}_p^{(\text{SL})}(k) = \|\mathbf{U}_{\text{SL}}\mathbf{a}\|_p \tag{22}$$

where

$$\mathbf{U}_{\text{SL}} = \left[\hat{\kappa}_s \mathbf{g}(\mathbf{d}, u_x^{(1)}, u_y^{(1)}) \cdots \hat{\kappa}_s \mathbf{g}(\mathbf{d}, u_x^{(K_s)}, u_y^{(K_s)})\right]^T, \quad \{u_x^{(i)}, u_y^{(i)}\} \in \Psi_{\text{SL}} \tag{23}$$

and $\hat{\kappa}_s$ is a discretization constant.

C. The Inverse White Noise Gain

To incorporate the WNG constraint in the optimization problem, it is more convenient to express it in terms of the inverse of the WNG. As such, for the kth iteration, the inverse WNG is given by

$$G_w^{-1} = \frac{(\mathbf{a}_k + \boldsymbol{\delta}_a)^T(\mathbf{a}_k + \boldsymbol{\delta}_a)}{|\mathbf{g}(\mathbf{d}, u_x^{(d)}, u_y^{(d)})^T(\mathbf{a}_k + \boldsymbol{\delta}_a)|^2} \tag{24}$$

The inverse WNG in (24) is nonconvex with respect to $\boldsymbol{\delta}_a$ since the denominator is nonconvex. To make the expression convex, we approximate (24) by setting the update $\boldsymbol{\delta}_a$ in the denominator to 0; i.e.,

$$G_w^{-1} \approx \frac{(\mathbf{a}_k + \boldsymbol{\delta}_a)^T(\mathbf{a}_k + \boldsymbol{\delta}_a)}{|\mathbf{g}(\mathbf{d}, u_x^{(d)}, u_y^{(d)})^T\mathbf{a}_k|^2} \tag{25}$$

Note that the approximation becomes more accurate as the optimization algorithm converges, and more or less equal upon convergence; this is because the L_2 norm of $\boldsymbol{\delta}_a$ is very small upon convergence, thereby making the denominator in (25) approximately equal to the denominator in (24).

D. Maximum Array-Length and Symmetric Arrays

The maximum length of the array along the x and y directions can be evaluated as

$$\begin{aligned} L_{xmax} &= \max_{i,j} \ [\max_{m,n} \ d_x(m,n) - d_x(i,j)] \\ L_{ymax} &= \max_{i,j} \ [\max_{m,n} \ d_y(m,n) - d_y(i,j)] \end{aligned} \tag{26}$$

In some applications, it may be desirable to ensure that the array coefficients are conjugate symmetric and the element positions are symmetric about the array center; i.e.,

$$a_{m,n} = \bar{a}_{M-m-1,N-n-1} \tag{27}$$

and

$$\begin{aligned} d_x(m,n) &= -d_x(M-m-1, N-n-1) \\ d_y(m,n) &= -d_y(M-m-1, N-n-1) \end{aligned} \tag{28}$$

where $\bar{a}_{m,n}$ is the complex conjugate of $a_{m,n}$.

III. The Optimization Problem

In this section, we develop formulations to minimize the number of elements in the array. We describe two variants. In the first variant, both the coefficients and positions of the elements are optimized, while in the second variant the positions are fixed and only the coefficients are optimized.

A. Variant 1

To reduce the number of elements in the array, the optimization problem can be formulated in so that the L_0 norm of the array coefficients is minimized under the constraint that the L_p norms of the mainlobe and sidelobe errors are below prescribed levels. Consequently, we have the optimization problem

$$\begin{aligned} \text{minimize} \quad & \|\mathbf{Sa}\|_0 && (29) \\ \text{subject to:} \quad & \mathbf{E}_p^{(\text{ML})} \le \Gamma_{\text{ML}} \\ & \mathbf{E}_p^{(\text{SL})} \le \Gamma_{\text{SL}} \\ & G_w^{-1} \le \Gamma_{wng}^{-1} && (30) \\ & && (31) \end{aligned}$$

where

$$\mathbf{S} = \begin{bmatrix} 1 & j & 0 & 0 & \cdots & 0 & 0 \\ 0 & 0 & 1 & j & \cdots & 0 & 0 \\ \vdots & \vdots & \vdots & \vdots & \ddots & \vdots & \vdots \\ 0 & 0 & 0 & 0 & \cdots & 1 & j \end{bmatrix} \tag{32}$$

and Γ_{ML}, Γ_{SL}, and Γ_{wng} are the prescribed thresholds for the mainlobe error, sidelobe error and WNG, respectively, and $\|x\|_0$ is the L_0 norm, i.e., the number of non-zero elements in x.

If the length of the array is also required to be less than a prescribed value, we can incorporate the constraints from (26) for the kth iteration; for e.g., if the maximum prescribed length of a linear array is Γ_l, the constraint can be expressed as

$$\max_i \ \{\max_m \ [d_x^{(k)}(m) + \delta_{d_x}(m)] - [d_x^{(k)}(i) + \delta_{d_x}(i)]\} \le \Gamma_l \tag{33}$$

To incorporate the symmetry constraints, the conditions in (27) and (28) for the kth iteration can be expressed as

$$a_{m,n}^{(k)} + \delta_{a_{m,n}} = \bar{a}_{M-m-1,N-n-1}^{(k)} + \bar{\delta}_{a_{M-m-1,N-n-1}} \tag{34}$$

and

$$\begin{aligned} d_x^{(k)}(m,n) + \delta_{d_x}(m,n) &= -[d_x^{(k)}(M-m-1, N-n-1) + \\ &\qquad \delta_{d_x}(M-m-1, N-n-1)] \\ d_y^{(k)}(m,n) + \delta_{d_y}(m,n) &= -[d_y^{(k)}(M-m-1, N-n-1) + \\ &\qquad \delta_{d_y}(M-m-1, N-n-1)] \end{aligned} \tag{35}$$

where $\delta_{a_{m,n}}$, $\delta_{d_x}(m,n)$, and $\delta_{d_y}(m,n)$ are the updates for $a_{m,n}^{(k)}$, $d_x^{(k)}(m,n)$, and $d_y^{(k)}(m,n)$, respectively, during the kth iteration. Note that the conditions in (34) and (35) are affine with respect to $\delta_{a_{m,n}}$, $\delta_{d_x}(m,n)$, and $\delta_{d_y}(m,n)$, and can therefore be incorporated into a convex optimization problem.

The optimization of the L_0 norm is a non-convex problem that is NP-hard and very difficult to solve even for moderate lengths. Therefore, to circumvent this we replace the L_0 norm by a re-weighted L_1 norm of the array coefficients [35]. To ensure that the maximum errors in the mainlobe and sidelobe regions are minimized we consider their L_∞ norm, that is, $\mathbf{E}_\infty^{(\mathrm{ML})}$ and $\mathbf{E}_\infty^{(\mathrm{SL})}$. Consequently, for the kth iteration, such an optimization problem is given by

$$\begin{aligned} \text{minimize} \quad & \|\mathbf{P}_k\ \mathbf{S}\ (\mathbf{a}_k + \boldsymbol{\delta}_a)\|_1 \\ \text{subject to:} \quad & \mathbf{E}_\infty^{(\mathrm{ML})}(\boldsymbol{\delta}_z, k) \le \Gamma_{\mathrm{ML}} \\ & \mathbf{E}_\infty^{(\mathrm{SL})}(\boldsymbol{\delta}_z, k) \le \Gamma_{\mathrm{SL}} \\ & G_w^{-1} \le \Gamma_{wng}^{-1} \\ & \|\boldsymbol{\delta}_z\|_2 \le \Gamma_\delta(k) \end{aligned} \tag{36}$$

where

$$\mathbf{z}_k^T = [\mathbf{a}_k^T\ \mathbf{d}_k^T] \tag{37}$$

$$\boldsymbol{\delta}_z^T = [\boldsymbol{\delta}_a^T\ \boldsymbol{\delta}_d^T] \tag{38}$$

$$\mathbf{P}_k = \mathrm{diag}\{\alpha_1^{(k)}, \ldots, \alpha_{NM}^{(k)}\} \tag{39}$$

$$\alpha_i^{(k)} = (\omega_i^{(k)} + \epsilon)^{-1} \tag{40}$$

$\boldsymbol{\delta}_z \in \mathbf{R}^{4MN}$ is the optimization variable, $\omega_i^{(k)}$ is the ith element in vector $\boldsymbol{\omega}_k = \mathbf{S}\mathbf{a}_k$, and ϵ is a small constant.

To speed up the convergence, $\Gamma_\delta(k)$ can be made relatively large during the starting iteration and gradually reduced to a small fixed value after a certain number of iterations. Furthermore, we found that adding a relaxation variable δ_{rlx} to Γ_δ facilitates faster convergence of the algorithm. Incorporating these modifications and substituting $\mathbf{E}_\infty^{(\mathrm{ML})}(k)$, $\mathbf{E}_\infty^{(\mathrm{SL})}(k)$, and G_w^{-1} by the expressions in (13), (20), and (25), respectively, the optimization problem becomes

$$\begin{aligned} \text{minimize} \quad & \|\mathbf{P}_k\ \mathbf{S}\ (\mathbf{a}_k + \boldsymbol{\delta}_a)\|_1 + V\delta_{rlx} \\ \text{subject to:} \quad & \|\mathbf{C}_k\boldsymbol{\delta}_z + \mathbf{f}_k\|_\infty \le \Gamma_{\mathrm{ML}} \\ & \|\mathbf{D}_k\boldsymbol{\delta}_z + \mathbf{g}_k\|_\infty \le \Gamma_{\mathrm{SL}} \\ & (\mathbf{a}_k + \boldsymbol{\delta}_a)^T(\mathbf{a}_k + \boldsymbol{\delta}_a) \le \Gamma_a(k) \\ & \|\boldsymbol{\delta}_z\|_2 \le \Gamma_\delta(k) + \delta_{rlx} \\ & \delta_{rlx} \ge 0 \end{aligned} \tag{41}$$

where $\boldsymbol{\delta}_z \in \mathbf{R}^{4MN}$ and $\delta_{rlx} \in \mathbf{R}^1$ are the optimization variables and

$$\Gamma_a(k) = \frac{|\mathbf{g}(\mathbf{d}, u_x^{(d)}, u_y^{(d)})^T\mathbf{a}_k|^2}{\Gamma_{wng}} \tag{42}$$

$$\Gamma_\delta(k) = \begin{cases} \gamma_k & k < T \\ \gamma_{small} & k \ge T \end{cases} \tag{43}$$

such that $\gamma_i > \gamma_{i+1}$ and $V > 0$. Note that the initial values of $\Gamma_\delta(k)$ cannot be made too large, otherwise the algorithm will be unstable; however, if it is made too small the algorithm will converge but will take more iterations. Typically, the starting value of $\Gamma_\delta(k)$ does not exceed 0.5 while the final value does not exceed 0.05. Though variations in $\Gamma_\delta(k)$ will change the speed of convergence, it does not usually affect the final solution, unless $\Gamma_\delta(k)$ is made exceedingly large.

The optimization problem in (41) can be readily expressed as a *second order cone programmming* (SOCP) problem as in [36] and solved using efficient SOCP solvers such as the one available in the SeDuMi optimization toolbox for MATLAB [37].

B. Variant 2

In the second variant, the positions of the elements are fixed and only the element coefficients are optimized. Therefore, we replace the mainlobe and sidelobe errors, $\mathbf{E}_\infty^{(\mathrm{ML})}(k)$ and $\mathbf{E}_\infty^{(\mathrm{SL})}(k)$, in (36) by $\hat{\mathbf{E}}_\infty^{(\mathrm{ML})}(k)$ and $\mathcal{E}_\infty^{(\mathrm{SL})}(k)$, respectively. Proceeding as in the previous subsection, and substituting $\hat{\mathbf{E}}_\infty^{(\mathrm{ML})}(k)$ and $\mathcal{E}_\infty^{(\mathrm{SL})}(k)$, by the expressions in (18) and (22), respectively, the optimization problem for the kth iteration is given by

$$\begin{aligned} \text{minimize} \quad & \|\mathbf{P}_k\ \mathbf{S}\ (\mathbf{a}_k + \boldsymbol{\delta}_a)\|_1 + V\delta_{rlx} \\ \text{subject to:} \quad & \|\hat{\mathbf{C}}_k\boldsymbol{\delta}_a + \hat{\mathbf{f}}_k\|_\infty \le \Gamma_{\mathrm{ML}} \\ & \|\mathbf{U}_{\mathrm{SL}}\ (\mathbf{a}_k + \boldsymbol{\delta}_a)\|_\infty \le \Gamma_{\mathrm{SL}} \\ & (\mathbf{a}_k + \boldsymbol{\delta}_a)^T(\mathbf{a}_k + \boldsymbol{\delta}_a) \le \Gamma_a(k) \\ & \|\boldsymbol{\delta}_a\|_2 \le \Gamma_\delta(k) + \delta_{rlx} \\ & \delta_{rlx} \ge 0 \end{aligned} \tag{44}$$

where $\boldsymbol{\delta}_a \in \mathbf{R}^{2MN}$ and $\delta_{rlx} \in \mathbf{R}^1$ are the optimization variables.

C. Special case for arrays having beampatterns with desired magnitude and phase

In some applications, it is necessary that the beampattern not only have a prescribed magnitude response but also a prescribed phase response. In such cases, the error described in (11) is not adequate, since only the magnitude error is minimized. To ensure that the phase error is also minimized, the beampattern error can be defined as

$$e_b(\mathbf{z}, u_x, u_y) = B(\mathbf{a}, \mathbf{d}, u_x, u_y) - B_d(u_x, u_y) \tag{45}$$

As in Section II-A, the L_p norm of the above error can be approximated for the kth iteration as

$$\mathbf{E}_p^{(\mathrm{BP})}(k) \approx \|\mathbf{H}_k\boldsymbol{\delta}_z + \mathbf{h}_k\|_p \tag{46}$$

where $\mathbf{H}_k$ and $\mathbf{h}_k$ is equivalent to (14) and (15), respectively, when $e_m(\mathbf{z}, u_x, u_y)$ is replaced by $e_b(\mathbf{z}, u_x, u_y)$ and Ψ_{ML} by Ψ_{BP}, which is the set of direction cosines for the prescribed beampattern.

For the case where the element positions are not optimized, the beampattern error is given by

$$\hat{e}_b(\mathbf{a}, u_x, u_y) = B(\mathbf{a}, \mathbf{d}, u_x, u_y) - B_d(u_x, u_y) \tag{47}$$

The L_p-norm of (47) can be expressed as a convex function given by

$$\mathcal{E}_p^{(\mathrm{BP})}(k) = \|\mathbf{W}_{\mathrm{BP}}\ \mathbf{a} - \mathbf{b}\|_p \tag{48}$$

where

$$\mathbf{W}_{\mathrm{BP}} = \left[\hat{\kappa}_b\mathbf{g}(\mathbf{d}, u_x^{(1)}, u_y^{(1)}) \cdots \hat{\kappa}_b\mathbf{g}(\mathbf{d}, u_x^{(K_b)}, u_y^{(K_b)})\right]^T \tag{49}$$

$$\mathbf{b} = \left[B_d(u_x^{(1)}, u_y^{(1)}) \cdots B_d(u_x^{(K_b)}, u_y^{(K_b)})\right]^T \tag{50}$$

and $\hat{\kappa}_b$ is a discretization constant and $\{u_x^{(i)}, u_y^{(i)}\} \in \Psi_{\mathrm{BP}}$.

D. Initialization Array

For faster convergence to a good solution, it is important to have a good initial estimate of $\mathbf{a}$ for the problems in (41) and (44). To derive the initialization array, we assume an array with fixed uniformly space element positions. For Variant 1 where the positions are also optimized, we set the element positions by uniformly distributing them across the prescribed 1-D or 2-D region. If Δ_x and Δ_y are the inter-element distances along the x and y directions, respectively, the positions of the elements along the x and y directions are given by

$$d_x(m,n) = p_x + m\Delta_x \quad \forall\ m \in [0, M-1] \tag{51}$$

$$d_y(m,n) = p_y + n\Delta_y \quad \forall\ n \in [0, N-1] \tag{52}$$

where p_x and p_y are the starting element positions along the x and y axis, respectively. To formulate a convex optimization problem for the initializing array, we constrain the array response in the mainlobe region to be real by canceling the imaginary component of the beampattern with a multiplying factor as was done in [38]; i.e., if

$$\eta(u_x,u_y) = \exp\left[-j\frac{2\pi}{\lambda}\left(\frac{N}{2}\Delta_x - p_x\right)u_x - \frac{2\pi}{\lambda}\left(\frac{M}{2}\Delta_y - p_y\right)u_y\right] \tag{53}$$

then it is straightforward to show that the product $\eta(u_x,u_y)B(u_x,u_y)$ will be real valued if (27) is satisfied and vice versa; this also implies that $|B(u_x,u_y)| = |\Re\{\eta(u_x,u_y)B(u_x,u_y)\}|$. Consequently, the beampattern-response error in the mainlobe region can be expressed as an absolute value of an affine function, which is convex. We then minimize the sidelobe error while maintaining the maximum mainlobe error within a prescribed level. A regularization term is also introduced to improve the conditioning of the problem. The resulting convex optimization problem is given by

$$\begin{aligned} \text{minimize} \quad & t + \lambda\|\mathbf{a}\|_2 \\ \text{subject to:} \quad & |\Re\{\eta(u_x,u_y)\mathbf{g}(\mathbf{d},u_x,u_y)^T\mathbf{a}\} - \\ & \ |B_d(u_x,u_y)|\ | \le \Gamma_{\text{ML}} \quad \forall\ \{u_x,u_y\} \in \Psi_{\text{ML}} \\ & \Im\{\mathbf{g}(\mathbf{d},u_x,u_y)^T\mathbf{a}\} = 0\ \forall\ \{u_x,u_y\} \in \Psi_{\text{ML}} \\ & |\mathbf{g}(\mathbf{d},u_x,u_y)^T\mathbf{a}| \le t \quad \forall\ \{u_x,u_y\} \in \Psi_{\text{SL}} \end{aligned} \tag{54}$$

$\mathbf{a} \in \mathbf{R}^{2MN}$ and $t \in \mathbf{R}^1$ are optimization variables, and λ is a positive value that typically lies between 0.0001 and 0.05. In our experiments, λ was set to 0.01. Note that the regularization term, $\lambda\|\mathbf{a}\|_2$, leads to a solution with smaller norm, which usually facilitates faster convergence to a good solution in the iterative optimization problems in (41) and (44). Furthermore, the smaller norm often results in an array with a larger WNG, thereby improving the robustness of the array.

Since the initialization array derived from (54) satisfies the conjugate symmetry in (27), it may not satisfy the inequality constraints in the optimization problems in (41) and (44) due to the reduced degrees-of-freedom from the conjugate symmetry. Therefore, to ensure that the initialization array always satisfies the constraints, we perform an additional optimization step by modifying the optimization problems in (41) and (44) to satisfy the inequality constraints, without minimizing the number of elements in the array. Consequently, for the case where the positions of the elements are optimized, such an optimization problem is given by

$$\begin{aligned} \text{minimize} \quad & t \\ \text{subject to:} \quad & \|\mathbf{C}_k\boldsymbol{\delta}_z + \mathbf{f}_k\|_\infty \le \Gamma_{\text{ML}} + t \\ & \|\mathbf{D}_k\boldsymbol{\delta}_z + \mathbf{g}_k\|_\infty \le \Gamma_{\text{SL}} + t \\ & (\mathbf{a}_k + \boldsymbol{\delta}_a)^T(\mathbf{a}_k + \boldsymbol{\delta}_a) \le \Gamma_a(k) + t \\ & \|\boldsymbol{\delta}_z\|_2 \le \Gamma_\delta(k) + t \\ & t \ge 0 \end{aligned} \tag{55}$$

where $t \in \mathbf{R}^1$ and $\boldsymbol{\delta}_z \in \mathbf{R}^{4MN}$ are optimization variables. Similarly, for the case where the positions of the elements are fixed, the optimization problem is given by

$$\begin{aligned} \text{minimize} \quad & t \\ \text{subject to:} \quad & \|\hat{\mathbf{C}}_k\boldsymbol{\delta}_a + \hat{\mathbf{f}}_k\|_\infty \le \Gamma_{\text{ML}} + t \\ & \|\mathbf{U}_{\text{SL}}\ (\mathbf{a}_k + \boldsymbol{\delta}_a)\|_\infty \le \Gamma_{\text{SL}} + t \\ & (\mathbf{a}_k + \boldsymbol{\delta}_a)^T(\mathbf{a}_k + \boldsymbol{\delta}_a) \le \Gamma_a(k) + t \\ & \|\boldsymbol{\delta}_a\|_2 \le \Gamma_\delta(k) + t \\ & t \ge 0 \end{aligned} \tag{56}$$

We can verify that the constraints in the optimization problem above are satisfied when we observe that t is very small and close to zero. In our experiments, we define $\Gamma_\delta(k)$ as

$$\Gamma_\delta(k) = \begin{cases} \gamma_k & k < 20 \\ 0.001 & k \ge 20 \end{cases} \tag{57}$$

where

$$\gamma_k = \gamma_1 - \frac{(\gamma_1 - \gamma_{19})(k-1)}{20-1} \tag{58}$$

$\gamma_1 = 0.1$ and $\gamma_{19} = 0.001$. If the constraints are feasible, t usually converges to a sufficiently small value (less that 10^{-5}) in less than 25 iterations.

We can therefore summarize the method for obtaining the initialization array in the following steps:

Step 1: Assuming an array with fixed element positions, solve the optimization problem in (54).

Step 2: Using the solution obtained from *Step 1* as the initialization array, solve the optimization problem in (55) if the element positions are optimized or the optimization problem in (56) if the element positions are fixed.

Note that if both the magnitude and phase of the desired beampattern is sought, the mainlobe and sidelobe errors in (55) and (56) are replaced by the beampattern error in (46) if the element positions are optimized or (48) if the positions are fixed.

E. Design Procedure

The overall design procedure for our proposed method can be described as follows:

Step 1: Determine the initialization array using the procedure in Section III-D. If the element positions are to be optimized, go to *Step 2*. Otherwise, for arrays with pre-defined element positions go to *Step 3*.

Step 2: The solution is obtained by solving the optimization problem in (41). The following optional constraints may also be incorporated in (41): (a) Array length constraint in (33); (b) Array-symmetry constraints in (34) and (35).

Step 3: The solution is obtained by solving the optimization problem in (44).

Note that for the special case where both the magnitude and phase errors of the beampattern need to be minimized, the mainlobe and sidelobe errors are replaced by the beampattern error in (46) for the optimization problems in *Steps 2* and *3*.

F. Practical Considerations

To evaluate the parameters that are dependent on the direction cosines, the 2-D non-uniform variable sampling (NVS) technique described in Appendix B of [41] is used. The 2-D technique results in a complexity reduction by more than an order of magnitude, thereby significantly speeding up the optimization algorithm. The weight V for the relaxation parameter, δ_{rlx}, in (41) and (44) should not be too small as this can make the optimization algorithm unstable and prevent it from converging; at the same time, it should also not be too large as this can slow down the convergence process. Typical values of V that have been found to work well range between 500 to 5000.

Though the convergence speed depends on the initialization point, in most cases the optimization algorithm in (41) converges to a good solution within 50 iterations. To ensure that the optimization is not prematurely terminated, we monitor the value of the objective function for about the last 5 iterations to check if it is not decreasing, as was done in [33].

In the design of arrays that have a focused beam, the objective is to maximize the directivity of the mainlobe rather than minimizing the mainlobe ripple: a straightforward approach is to constrain the beampattern to unity in the direction of the focused beam. To do this in the optimization problems in (41), (44), and (54), we simply evaluate the mainlobe error only along the direction of the focused beam while setting Γ_{ML} to zero.

IV. Numerical Results

In this section, we provide comparative experimental results to demonstrate the efficiency of the proposed method. Eight examples of various array designs are considered. In Examples 1 to 3 we compare linear arrays with optimized element positions whereas in Examples 4 and 5 we compare linear arrays with both fixed and optimized element positions. In Examples 6 and 7 we compare linear arrays with optimized element positions where both the magnitude and phase of the desired beampattern is sought. Then in Example 8, we compare planar arrays with both fixed and optimized element positions.

Depending on whether the positions of the elements are fixed or optimized, we have the following design variants for the proposed method:

1) Design P1-A: This design corresponds to the first variant of the proposed method where both the array coefficients and positions of the elements are optimized. The solution is obtained by solving the iterative optimization problem in (41). The initialization array for the iterative optimization problem is obtained using the procedure in Section III-D.

2) Design P1-B: This design corresponds to the second variant of the proposed method where only the array coefficients are optimized and the positions of the elements are fixed at predefined values. The solution is obtained by solving the iterative optimization problem in (44). The initialization array for this variant is also obtained using the procedure in Section III-D.

3) Design P2-A: This design corresponds to the special case where both the magnitude and phase of the prescribed beampattern is optimized. In this design both the array coefficients and the positions of the elements are optimized. The solution is obtained by solving a modified version of the iterative optimization problem in (41), where the mainlobe and sidelobe errors are replaced by the beampattern error in (46) with $p = \infty$. The initialization array for this design is obtained using the procedure in Section III-D.

4) Design P2-B: This design corresponds to the special case where both the magnitude and phase of the prescribed beampattern is sought. In this design only the array coefficients are optimized. The solution is obtained by solving a modified version of the iterative optimization problem in (44), where the mainlobe and sidelobe errors are replaced by the beampattern error in (48) with $p = \infty$. The initialization array for this design is obtained using the procedure in Section III-D.

In all four variants above, unless explicitly stated, the WNG constraint is not applied; this is done by setting Γ_{wng} to 0 or removing the WNG constraint from the optimization problem. Furthermore, in some of the experiments we also compare design extensions of P1-A by incorporating various combinations of the WNG constraint, array-length constraint, and array-symmetry constraint, which are indicated in the comparison tables using the following abbreviations:

WC: Corresponds to the WNG constraint where the minimum WNG, in dB, is Γ_{wng}^{dB}.

ALC: Corresponds to array-length constraint in (33) where the maximum array length is Γ_l.

SC: Corresponds to the symmetry constraints in (34) and (35).

In all of the examples, the elements were assumed to be isotropic and the value of ϵ in (40) was set to 10^{-5}. For the iterative optimization problem in (41), V was set to 1000 and $\Gamma_\delta(k)$ defined as in (57). The active elements were selected by considering only those elements with coefficient magnitudes greater than 10^{-5}; coefficients with magnitudes less than or equal to 10^{-5} were set to 0.

For the linear array, the angle-dependent parameters for the iterative optimization problems in (41) and (44) were evaluated using the NVS technique in [32] where the number of virtual and actual sampling points between 0° and 180° were 70 and 2000, respectively, and near the edges of the mainlobe and sidelobe regions, 6 of the virtual sampling points were fixed as actual sampling points. Whereas for the planar arrays, the

direction-cosine dependent parameters were evaluated using the 2-D NVS technique described in Appendix B of [41], where the number of virtual and actual sampling points in the direction-cosine plane were 400 and 300000, respectively. Near the edges of the mainlobe and the sidelobe regions, the sampling points were fixed and correspond to the last 3 virtual sampling points before the edges.

The nonuniform sampling technique is applicable only if the optimization problem is iterative. Hence, for designs that are based on solving a non-iterative convex optimization problem, uniform sampling was used instead. Consequently, for the optimization problem in (54) the number of sampling points along each of the two dimensions was set to 200.

The array performance is evaluated using the following parameters:

Maximum Mainlobe ripple: The parameter is defined as

$$A_{\max}^{(\mathrm{ML})} = 20 \log \frac{M_{\max}^{(\mathrm{ML})}}{M_{\min}^{(\mathrm{ML})}} \tag{59}$$

where

$$M_{\max}^{(\mathrm{ML})} = \max_{\{u_x,u_y\}\in\Psi_{\mathrm{ML}}} |B(u_x,u_y)| \tag{60}$$

$$M_{\min}^{(\mathrm{ML})} = \min_{\{u_x,u_y\}\in\Psi_{\mathrm{ML}}} |B(u_x,u_y)| \tag{61}$$

Minimum sidelobe attenuation: The minimum sidelobe attenuation is defined as the negative of the maximum sidelobe gain, given by

$$A_{\min}^{(\mathrm{SL})} = -20 \log M_{\max}^{(\mathrm{SL})} \tag{62}$$

where

$$M_{\max}^{(\mathrm{SL})} = \max_{\{u_x,u_y\}\in\Psi_{\mathrm{SL}}} |B(u_x,u_y)| \tag{63}$$

Maximum error of the beampattern: The maximum error of the beampattern is defined as

$$E_{\max}^{(\mathrm{BP})} = \max_{\{u_x,u_y\}\in\Psi_{\mathrm{BP}}} |B(u_x,u_y) - B_d(u_x,u_y)| \tag{64}$$

White Noise Gain: The WNG is used for evaluating the robustness of the array. It is defined in (10).

To ensure a fair comparison, the maximum gain of the beampattern in our experiments have been normalized to 1. Note also that the computation of the performance parameters and beampattern plots in our experiments was done by considering only the active elements.

In Section IV-A to IV-C below, we compare the proposed design method with several state-of-the-art methods for the design of minimum element arrays including the methods in [12], [13], [14], [15], [16], [17], and [40]. The plots of all linear-array coefficients corresponding to the proposed designs are included in [41].

A. Examples 1-3: Linear Arrays with Optimized Element Positions

In this subsection, we consider linear array designs where the elements can lie at arbitrary positions. Therefore, for the proposed method, we consider Design P1-A where both the array coefficients and element positions are optimized. The competing designs for Examples 1, 2, and 3 correspond to the first example in [16], first example in [13], and the last example in [14]. The required design specifications for the array designs are given in Tables I, III, and V, respectively. In Example 1, the array is required to have a focused beam with asymmetric sidelobe attenuation levels. The competing design in [16] ensured that the array length was less than 9.7λ and the sidelobe levels were less than -29.8 dB and -19.8 dB on either side. On the other hand, in Examples 2 and 3 the arrays are required to have flat-top beampatterns. Example 2, in addition, has two sidelobe regions, A and B, each requiring different attenuation levels. The competing designs in Example 2 and 3 ensured that the maximum passband ripple and minimum stopband attenuation were within prescribed levels; however, in both designs, no array length or robustness constraints were imposed.

TABLE I
DESIGN SPECIFICATIONS FOR EXAMPLE 1 OF A LINEAR ARRAY THAT HAS A FOCUSED BEAM WITH ARBITRARY ELEMENT POSITIONS

Parameters	Values
Element positions	arbitrary
Main beam direction, $(\sin\theta - \sin\theta_d)$	0
Sidelobe region, $(\sin\theta - \sin\theta_d)$	$[-2,-0.12]$ $\cup$ $[2,0.12]$
Minimum sidelobe atten. (left) (dB)	20
Minimum sidelobe atten. (right) (dB)	30

[1] Derived from the coefficients of the competing array in [16]

TABLE II
DESIGN RESULTS FOR EXAMPLE 1 FOR LINEAR ARRAYS WITH ARBITRARY ELEMENT POSITIONS

Parameters	Design P1-A	Method in [16]
$A_{\min}^{(\mathrm{SL})}$ (left), dB	22.3	21.34
$A_{\min}^{(\mathrm{SL})}$ (right), dB	31.31	30.31
Array length, λ	9.6	9.66
WNG, dB	12.87	12.84
No. of elements	22	22

From Table II and Fig. 1, we observe that although both the proposed and competing designs in Example 1 have the same number of elements, the proposed design has greater sidelobe attenuations, shorter array length, and slightly greater WNG.

In Example 2, we compare the proposed design, P1-A, with the competing design. In addition, we also include two

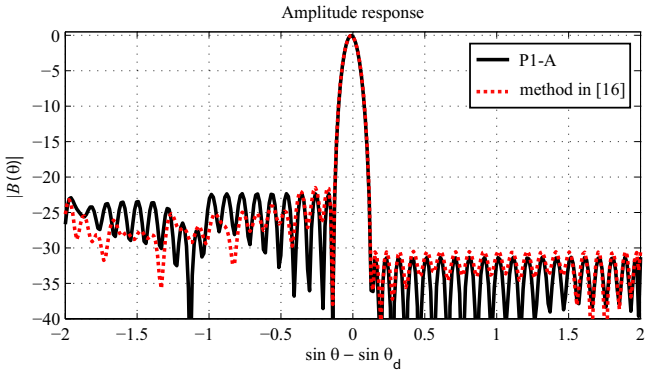

Fig. 1. Beampattern plots of the arrays in Example 1 that are obtained using Design P1-A (black curve) and the method in [16] (red dotted curve).

TABLE III
DESIGN SPECIFICATIONS FOR EXAMPLE 2 OF A LINEAR ARRAY WITH FLAT-TOP BEAMPATTERN AND ARBITRARY ELEMENT POSITIONS

Parameters	Values
Element positions	arbitrary
Mainlobe region, Ψ_{ML}, (deg)[2]	$[78.7^\circ - 101.4^\circ]$
Sidelobe region A, Ψ_{SL}, (deg)[2]	$[64.3^\circ - 71.4^\circ] \cup [108.6^\circ - 115.8^\circ]$
Sidelobe region B, Ψ_{SL}, (deg)[2]	$[0^\circ - 64.3^\circ] \cup [115.8^\circ - 180^\circ]$
Max. Mainlobe ripple (dB)	2
Min. sidelobe atten. (region A) (dB)	39
Min. sidelobe atten. (region B) (dB)	20

[2] Derived from the coefficients of the competing array in [13]

TABLE IV
DESIGN RESULTS FOR EXAMPLE 2 WHERE THE ELEMENT POSITIONS IN THE PROPOSED METHOD ARE OPTIMIZED

Parameters	Design P1-A	Method in [13]
$A_{\max}^{(\mathrm{ML})}$, dB	1.84	1.84
$A_{\min}^{(\mathrm{SL})}$ (region A), dB	41.42	39.8
$A_{\min}^{(\mathrm{SL})}$ (region B), dB	22.32	20.51
Array length, λ	10.6	7.85
WNG, dB	5.16	5.31
No. of active elements	10	12
Parameters	Design P1-A (WC, ALC) $\Gamma_{wng}^{(\mathrm{dB})} = 5.31$ $\Gamma_l = 7.85$	Design P1-A (ALC) $\Gamma_l = 7.85$
$A_{\max}^{(\mathrm{ML})}$, dB	1.84	1.84
$A_{\min}^{(\mathrm{SL})}$ (region A), dB	40.29	40.29
$A_{\min}^{(\mathrm{SL})}$ (region B), dB	21.11	21.12
Array length, λ	7.85	7.85
WNG, dB	5.4	5.09
No. of active elements	12	11

extensions of P1-A where (1) the maximum array length is constrained to be less than that of the competing design; and (2) the maximum array length is less than that of the competing design and the WNG is greater than that of the competing design. The results of the comparison are given in Table IV and Fig. 2; for the two extensions of P1-A, the beampattern plots are included in [41]. From Table IV and the corresponding plots, we observe that the proposed designs have better mainlobe ripple and sidelobe attenuation while the number of elements are equal to or less than that for the competing design. In Example 3, we again observe that the proposed designs have better mainlobe ripple and sidelobe attenuation while the number of elements are equal to or less than that of the competing design.

In both Examples 2 and 3, it is interesting to observe that

TABLE V
DESIGN SPECIFICATIONS FOR EXAMPLE 3 OF A LINEAR ARRAY WITH FLAT-TOP BEAMPATTERN AND ARBITRARY ELEMENT POSITIONS

Parameters	Values
Element positions	arbitrary
Mainlobe region, Ψ_{ML}, (deg)[3]	$[72.2^\circ - 107.8^\circ]$
Sidelobe region, Ψ_{SL}, (deg)[3]	$[0^\circ - 63^\circ] \cup [117.2^\circ - 180^\circ]$
Maximum mainlobe ripple (dB)	1.4
Minimum sidelobe attenuation (dB)	35

[3] Derived from the coefficients of the competing array in [14]

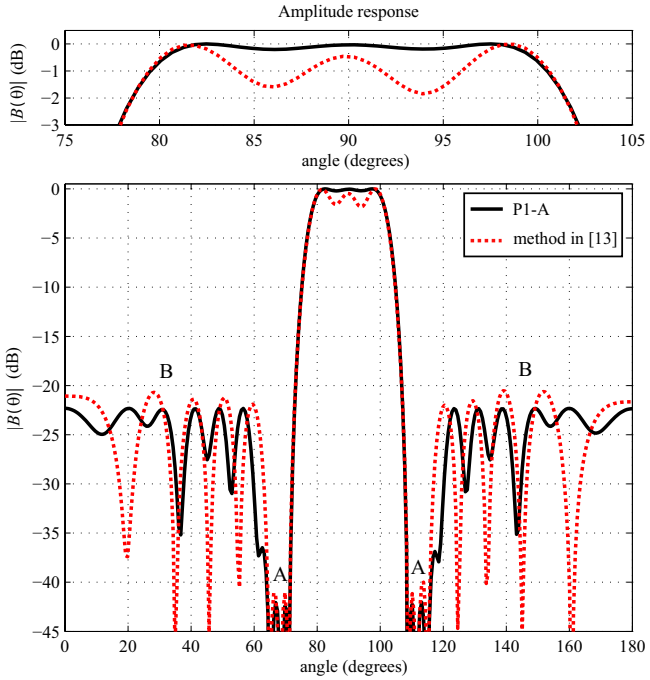

Fig. 2. Beampattern plots of the arrays in Example 2 that are obtained using Design P1-A (black curve) and the method in [13] (red dotted curve). The sidelobe regions A and B are also indicated in the plots.

TABLE VI
DESIGN RESULTS FOR EXAMPLE 3 WHERE THE ELEMENT POSITIONS IN THE PROPOSED METHOD ARE OPTIMIZED

Parameters	Design P1-A	Design P1-A (WC, ALC) $\Gamma_{wng}^{(\mathrm{dB})} = 2.9$ $\Gamma_l = 6.94$	Method in [14]
$A_{\max}^{(\mathrm{ML})}$, dB	1.37	1.37	1.37
$A_{\min}^{(\mathrm{SL})}$, dB	40.06	37.63	36.33
Array length, λ	8.84	6.87	6.94
WNG, dB	3.8	3	2.90
No. of elements	9	10	10

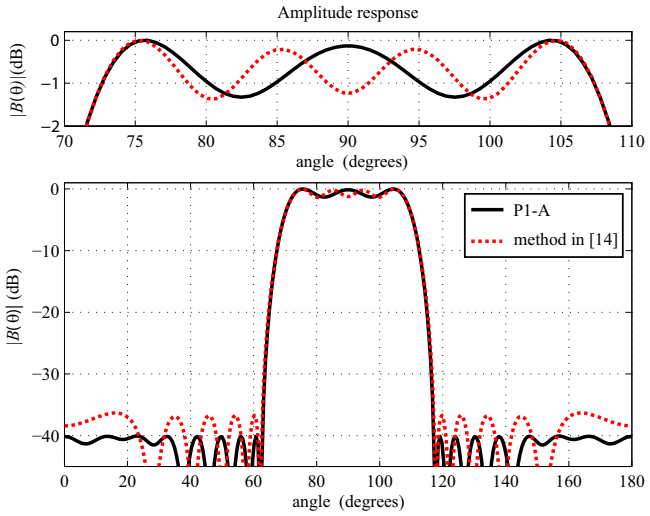

Fig. 3. Beampattern plots of the arrays in Example 3 that are obtained using Design P1-A (black curve) and the method in [14] (red dotted curve).

TABLE VII
DESIGN SPECIFICATIONS FOR EXAMPLE 4 OF A LINEAR ARRAY WITH FLAT-TOP BEAMPATTERN HAVING ELEMENTS AT PREDEFINED OR ARBITRARY POSITIONS

Parameters	Values
Mainlobe region, Ψ_{ML}, (deg)[4]	$[70^\circ - 110^\circ]$
Sidelobe region, Ψ_{SL}, (deg)[4]	$[0^\circ - 65^\circ] \cup [115^\circ - 180^\circ]$
Maximum mainlobe ripple (dB)	0.5
Minimum sidelobe attenuation (dB)	30

[4] Same as in [15]

when the WNG and/or the array length are not constrained, the number of elements of the proposed design becomes smaller than that of the competing design, which implies that the reduction in elements is obtained at the expense of a decrease in WNG or an increase in array length.

B. Examples 4-5: Linear Arrays With Predefined or Optimized Positions

In this subsection, we consider linear arrays where the elements are confined to either predefined or arbitrary positions. Therefore, for the proposed method we consider both Designs P1-A and P1-B. The competing designs for Examples 4 and 5 correspond to the first example in [15] and first example in [40]. The required design specifications for the array designs are given in Tables VII and IX, respectively. For arrays where the positions of the elements are fixed, the elements are located at positions that are multiples of 0.5λ for both Examples 4 and 5.

The competing designs in both Examples 4 and 5 ensured that the maximum mainlobe ripple and minimum sidelobe attenuation were within prescribed levels. In both the designs, the elements were located at predefined positions and no robustness constraint was imposed.

For the proposed designs with optimized element positions, the initialization array for Example 4 has 50 elements with a uniform spacing of 0.5λ between the elements while the initialization array for Example 5 has 20 elements with the same uniform spacing.

In Examples 4 and 5, we compare designs P1-A and P1-B with the competing designs. We also include two extensions of design P1-A for Examples 4 and 5 that have additional constraints. In Example 4, the two extensions have constraints to ensure that (1) the WNG of P1-A is greater than that of design P1-B; and (2) the WNG of P1-A is greater than that of the P1-B, the array coefficients are conjugate symmetric, and the element coefficients are symmetrical about the array center. In Example 5, the two extensions have constraints to ensure that (1) the array length is less than that of the competing design; and (2) the array length is less than that of the competing design and the WNG is greater than that of the competing design. The comparison results for Examples 4 and 5 are given in Tables VIII and X, and Figs. 4 and 5. The beampattern plots for the design extensions of P1-A are included in [41].

From Tables VIII and X and the corresponding plots, we observe that the proposed designs in Examples 4 and 5 have smaller mainlobe ripple, greater sidelobe attenuation,

TABLE VIII
DESIGN RESULTS FOR EXAMPLE 4 OF LINEAR ARRAYS WITH FIXED AND OPTIMIZED ELEMENT POSITIONS

Parameters	Design P1-A	Design P1-B	Method in [15]
$A_{\text{max}}^{(\text{ML})}$, dB	0.441	0.442	0.446
$A_{\text{min}}^{(\text{SL})}$, dB	30.2	31.2	30
Array length, λ	17.11	18.5	NP
WNG, dB	3.25	4.48	NP
No. of active elements	15	27	31
Parameters	**Design P1-A (SC, WC) $\Gamma_{wng}^{(\text{dB})} = 4.48$**	**Design P1-A (WC) $\Gamma_{wng}^{(\text{dB})} = 4.48$**	**Method in [15]**
$A_{\text{max}}^{(\text{ML})}$, dB	0.441	0.441	0.446
$A_{\text{min}}^{(\text{SL})}$, dB	30.2	31.2	30
Array length, λ	16.84	17.16	NP
WNG, dB	4.48	4.48	NP
No. of active elements	17	16	31

NP: not provided

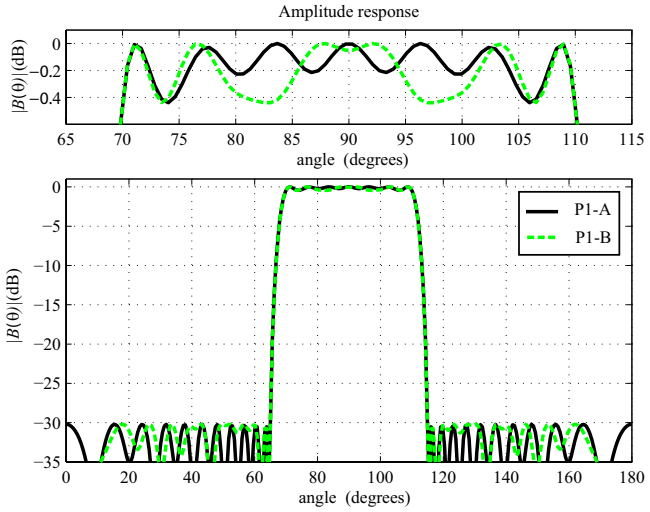

Fig. 4. Beampattern plots of the arrays in Example 4 that are obtained using Design P1-A (black curve) and Design P1-B (green dashed curve). Note that we are unable to plot the beampattern of the competing array in [15] since the coefficients were not provided.

TABLE IX
DESIGN SPECIFICATIONS FOR EXAMPLE 5 OF A LINEAR ARRAY WITH FLAT-TOP BEAMPATTERN HAVING ELEMENTS AT PREDEFINED OR ARBITRARY POSITIONS

Parameters	Values
Mainlobe region, Ψ_{ML}, (deg)[5]	$[73.6^\circ - 108.3^\circ]$
Sidelobe region, Ψ_{SL}, (deg)[5]	$[0^\circ - 64.1^\circ] \cup$ $[117.9^\circ - 180^\circ]$
Maximum mainlobe ripple (dB)	1.2
Minimum sidelobe attenuation (dB)	34

[5] Derived from the coefficients of the competing array in [40]

TABLE X
DESIGN RESULTS FOR EXAMPLE 5 OF LINEAR ARRAYS WITH FIXED AND OPTIMIZED ELEMENT POSITIONS.

Parameters	Design P1-A	Design P1-B	Method in [40]
$A_{\max}^{(\mathrm{ML})}$, dB	1.16	1.16	1.17
$A_{\min}^{(\mathrm{SL})}$, dB	35.58	35.64	35.45
Array length, λ	7.68	7	7
WNG, dB	4.42	4.12	4.07
No. of active elements	10	14	15
Parameters	Design P1-A (WC, ALC) $\Gamma_{wng}^{(\mathrm{dB})} = 4.07$ $\Gamma_l = 7$	Design P1-A (ALC) $\Gamma_l = 7$	Method in [40]
$A_{\max}^{(\mathrm{ML})}$, dB	1.16	1.16	1.17
$A_{\min}^{(\mathrm{SL})}$, dB	35.64	35.64	35.45
Array length, λ	6.87	7	7
WNG, dB	4.15	2.89	4.07
No. of active elements	11	10	15

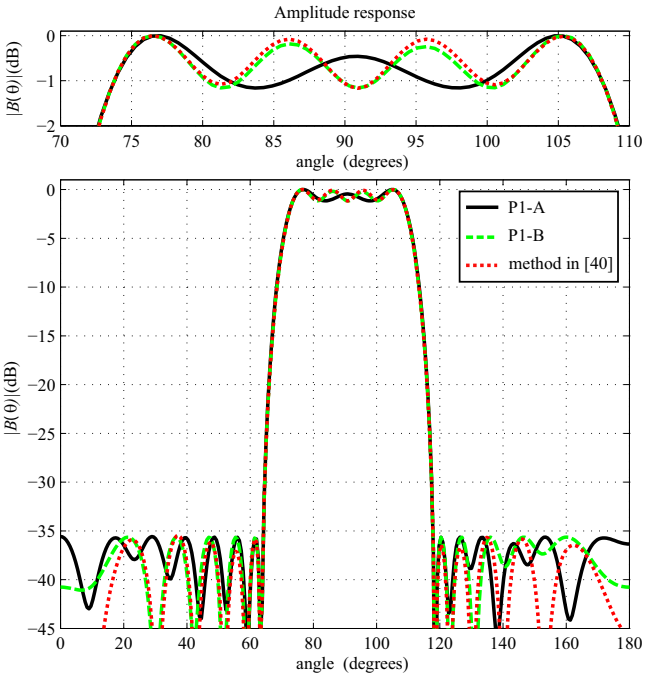

Fig. 5. Beampattern plots of the arrays in Example 5 that are obtained using Design P1-A (black curve), Design P1-B (green dashed curve), and the method in [40] (red dotted curve).

and smaller or equal number of elements than the competing designs. We also observe that imposing additional constraints, such as constraints on the minimum WNG, maximum array length, conjugate symmetry of the coefficients, or symmetry of the element positions, tends to reduce the degrees of freedom in the optimization thereby leading to an increase in the number of elements in the proposed design.

C. Examples 6-7: Chebyshev Linear Arrays With Optimized Element Positions

In this subsection, we consider linear arrays where both the gain and phase of the prescribed beampattern is sought. For comparison, we consider competing designs from the first example in [17] and the first example in [12], and compare them with design P2-A. The prescribed beampattern in both examples corresponds to a 20-element uniformly spaced Chebyshev array as described in Section III-A of [17].

To evaluate the performance of the various designs we compare the number of elements, the maximum and RMSE error of the beampattern, and the WNG between the various designs. The competing design for Example 6 was obtained by minimizing the L_1 norm of the array coefficients while constraining the L_2 norm of the beampattern error to be below a prescribed threshold. For Example 7, the competing design was obtained by using the matrix pencil method whereby the beampattern error was constrained to be below a prescribed threshold in the least-squares sense.

The required design specifications, results, and plots for the two examples are included in [41]. From the design results and plots, we observe that the proposed designs in Examples 6 and 7 have greater WNG, smaller beampattern error and smaller array length than the competing designs. In Example 6, the proposed design has one less element than the competing design, while in Example 7 the proposed and competing designs have the same number of elements.

TABLE XI
DESIGN SPECIFICATIONS FOR EXAMPLE 8 OF A PLANAR ARRAY WITH FLAT-TOP BEAMPATTERN HAVING ELEMENTS AT PREDEFINED OR ARBITRARY POSITIONS

Parameters	Values
Mainlobe region, Ψ_{ML}	$u_x^2 + u_y^2 < 0.2^2$
Sidelobe region, Ψ_{SL}	$u_x^2 + u_y^2 > 0.4^2$, $\lvert u_x\rvert < 1, \lvert u_y\rvert < 1$
Maximum mainlobe ripple (dB)	1.5
Minimum sidelobe attenuation (dB)	25

D. Examples 8: Planar Arrays With Predefined or Optimized Positions

Here we consider the design of a planar array where the elements are confined to either predefined or arbitrary positions. For the proposed method, we compare both Designs P1-A and P1-B. The competing array in this example corresponds to the seventh example in [15]. The competing design was obtained by ensuring that the maximum mainlobe ripple and mininum sidelobe attenuation were within prescribed levels, and the elements were confined to predefined positions. For Design P1-A, the initializing array has 11×11 elements that are located on a square grid with inter-element spacing of 0.5λ. We also included an extension of design P1-A where the array coefficients are constrained to be conjugate symmetric and the element positions are constrained to be symmetric about the origin. The complete design specifications are given in Table XI.

The design results, beampattern plots, and element positions are given in Table XII, and Figs. 6, 7, 8, and 9. For the design extension of P1-A, the beampattern plots and elements positions are included in [41]. From the tables and plots, we observe that the proposed designs have smaller number of elements and equal or better mainlobe ripple and sidelobe attenuation than the competing design. As in Examples 4 and

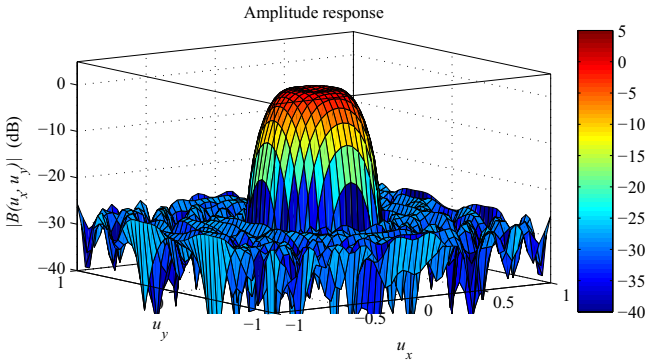

Fig. 6. Beampattern plot of the array in Example 8 that is obtained using Design P1-A.

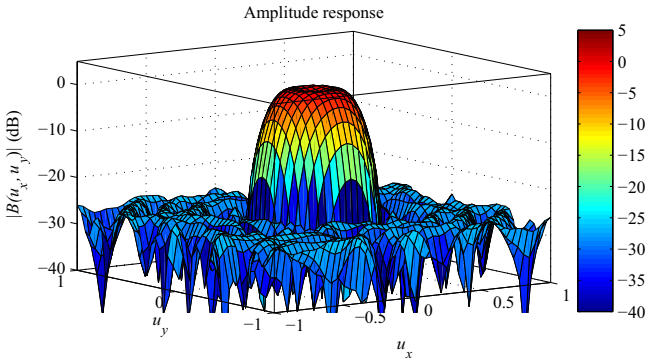

Fig. 7. Beampattern plot of the array in Example 8 that is obtained using Design P1-B.

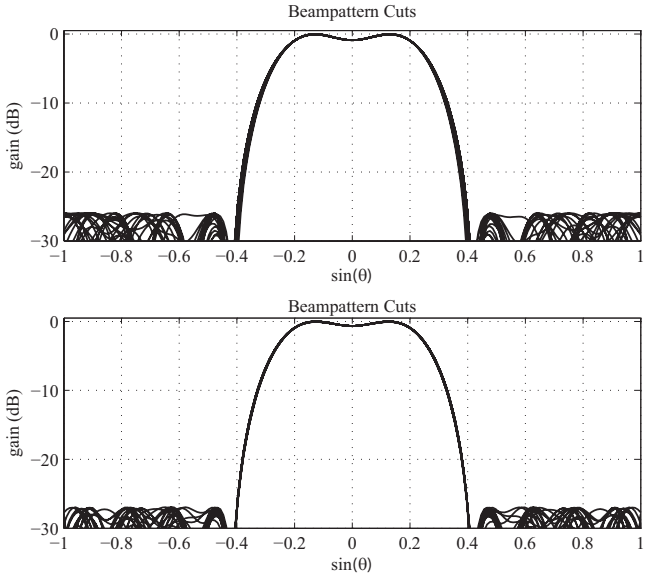

Fig. 8. Plots of beampattern cuts of the planar arrays in Example 8 for 20 uniformly sampled values of ϕ in the range $[0, \pi]$, for Design P1-A (top) and Design P1-B (bottom).

TABLE XII
DESIGN RESULTS FOR EXAMPLE 8 FOR A PLANAR ARRAY.

Parameters	Design P1-B	Design in [15]
$A_{\max}^{(ML)}$, dB	0.99	1
$A_{\min}^{(SL)}$, dB	25.93	25.85
WNG, dB	11.91	NP
No. of active elements	78	85
Parameters	Design P1-A	Design P1-A (SC)
$A_{\max}^{(ML)}$, dB	0.97	0.98
$A_{\min}^{(SL)}$, dB	26.24	26.33
WNG, dB	10.57	11.26
No. of active elements	55	61

NP: not provided

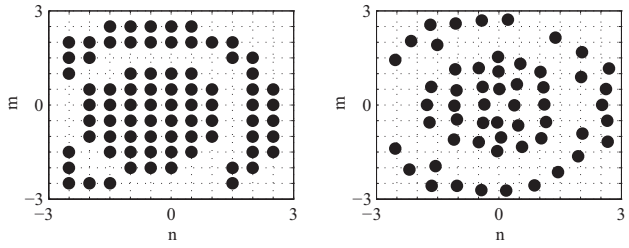

Fig. 9. Plots of positions of the active elements for Example 8 that are obtained using Design P1-A (left) and Design P1-B (right).

5, design P1-A has a smaller number of elements than design P1-B.

The above design examples have shown that the proposed design method yields arrays with minimum number of elements when compared with competing methods, while at the same time providing the flexibility of controlling the array dimensions, WNG, and symmetry characteristics of the array. It should be pointed out that the optimization of the magnitude response and element positions is nonlinear and nonconvex and therefore the solution obtained sometimes depends on the initialization array used, which implies that global convergence cannot be guaranteed. In effect, the proposed method gives quality suboptimal designs that may sometimes be globally optimal.

The optimization problems in the examples were solved on a computer running an Intel Core i7-640LM processor using the SeDuMi optimization toolbox for MATLAB [37]. For the planar array, the proposed iterative optimization method takes anywhere between 10 to 40 minutes to compute while for the linear array it takes less than 5 minutes.

V. CONCLUSIONS

A new method for the synthesis of linear and planar arrays having arbitrary beamwidth and sidelobe levels was proposed. In the method, the number of elements in an array is minimized while constraining the amplitude-response error in the mainlobe region and the attenuation in the sidelobe region within prescribed levels. To ensure robustness of the array, we constrain a sensitivity parameter, namely, the white noise gain, to be above a prescribed level. Furthermore, the method also provides the additional flexibility of controlling the array dimensions, symmetry properties, and element positions. The

problem is solved as an iterative constrained optimization problem where the amplitude-response error is approximated using a linear update at each iteration while concurrently minimizing a re-weighted L_1 norm of the array coefficients. Two variants of the method have been described. In the first variant, both the array coefficients and the positions of the elements are optimized while in the second variant only the array coefficients are optimized and the elements are fixed at predefined positions. Experimental comparisons with several state-of-the-art competing methods showed that the proposed method provides greater flexibility of controlling the robustness, beampattern response error, array dimensions, and element positions while at the same time the number of elements is less than or equal to that of the competing methods.

ACKNOWLEDGMENT

The authors are grateful to the Natural Sciences and Engineering Research Council of Canada for supporting this work.

REFERENCES

[1] H. Unz, "Linear arrays with arbitrarily distributed elements," *IEEE Trans. Antennas Propag.*, vol. 8, pp. 222-223, 1960.

[2] R. F. Harrington, "Sidelobe reduction by non-uniform element spacing," *IRE Trans. Antennas Propag.*, vol. 9, pp. 187-192, 1961.

[3] R. E. Willey, "Space tapering of linear and planar arrays," *IRE Trans. Antenna Propag.*, vol. 10, pp. 369-377, 1962.

[4] M. Skolnik, G. Nemhauser, and J. Sherman, III, "Dynamic programming applied to unequally spaced arrays," *IEEE Trans. Antennas Propag.*, vol. 12, no. 1, pp. 35-43, 1964.

[5] A. Ishimaru and Y.-S. Chen, "Thinning and broadbanding antenna arrays by unequal spacings," *IEEE Trans. Antennas Propag.*, vol. 13, no. 1, pp. 34-42, 1965.

[6] Y. T. Lo, "A study of space-tapered arrays," *IEEE Trans. Antennas Propag.*, vol. 14, no. 2, pp. 22-30, 1966.

[7] M. I. Skolnik, "Ch. Nonuniform arrays," in *Antenna Theory*, R. E. Collin and F. Zucker, Eds. New York: McGraw-Hill, 1969, pt. I.

[8] B. P. Kumar and G. R. Branner, "Synthesis of unequally spaced arrays using Legendre series expansion," in *Proc. IEEE Antennas Propag. Int. Symp.*, 1997, vol. 4, pp. 2236-2239.

[9] D. G. Leeper, "Isophoric arrays - Massively thinned phased arrays with well controlled sidelobes," *IEEE Trans. Antennas Propag.*, vol. 47, no. 12, pp. 1825-1835, 1999.

[10] D. G. Kurup, M. Himdi, and A. Rydberg, "Synthesis of uniform amplitude unequally spaced antenna arrays using the differential evolution algorithm," *IEEE Trans. Antennas Propag.*, vol. 51, pp. 2210-2217, 2003.

[11] O. Quevedo-Teruel and E. Rajo-Iglesias, "Ant colony optimization for array synthesis," in *Proc. IEEE Antennas Propag. Society Int. Symp.*, July 9-14, 2006, pp. 3301-3304.

[12] Y. Liu, Z. Nie, and Q. H. Liu, "Reducing the number of elements in a linear antenna array by the Matrix Pencil Method," *IEEE Trans. Antennas Propag.*, vol. 56, no. 9, pp. 2955-2962, Sep. 2008.

[13] Y. Liu, Z. Nie, and Q. H. Liu, "A new method for the synthesis of non-uniform linear arrays with shaped power patterns," *Progr. Electromagn. Res.*, vol. 107, pp. 349-363, 2010.

[14] Y. Liu, Q. H. Liu, and Z. Nie, "Reducing the number of elements in the synthesis of shaped-beam patterns by the forward-backward matrix pencil method," *IEEE Trans. Antennas Propag.*, vol. 58, no. 2, pp. 604-608, Feb. 2010.

[15] S. E. Nai, W. Ser, Z. L. Yu, and H. Chen, "Beampattern synthesis for linear and planar arrays with antenna selection by convex optimization," *IEEE Trans. Antennas Propag.*, vol. 58, no. 12, pp. 3923-3930, Dec. 2010.

[16] B. Fuchs, "Synthesis of sparse arrays with focused or shaped beampattern via sequential convex optimizations," *IEEE Trans. Antennas Propag.*, vol. 60, no. 7, pp. 3499-3503, Jul. 2012.

[17] W. Zhang, L. Li, and F. Li, "Reducing the number of elements in linear and planar antenna arrays with sparseness constrained optimization," *IEEE Trans. Antennas Propag.*, vol. 59, no. 8, pp. 3106-3111, Jul. 2011.

[18] G. Oliveri, M. Carlin, and A. Massa, "Complex-weight sparse linear array synthesis by bayesian compressive sampling," *IEEE Trans. Antennas Propag.*, vol. 60, no. 5, pp. 2309-2326, May. 2012.

[19] G. Oliveri and A. Massa, "Bayesian compressive sampling for pattern synthesis with maximally sparse non-uniform linear arrays," *IEEE Trans. Antennas Propag.*, vol. 59, no. 2, pp. 467-481, Feb. 2011.

[20] F. Viani, G. Oliveri, and A. Massa, "Compressive sensing pattern matching techniques for synthesizing planar sparse arrays," *IEEE Trans. Antennas Propag.*, vol. 61, no. 9, pp. 4577-4587, Sept. 2013.

[21] G. Oliveri, E. T. Bekele, F. Robol, and A. Massa, "Sparsening conformal arrays through a versatile BCS-based method," *IEEE Trans. Antennas Propag.*, vol. 62, no. 4, pp. 1-9, Apr. 2014.

[22] G. Oliveri, L. Manica, and A. Massa, "ADS-Based guidelines for thinned planar arrays," *IEEE Trans. Antennas Propag.*, vol. 58, no. 6, pp. 1935-1948, Jun. 2010.

[23] G. Oliveri, F. Caramanica, C. Fontanari, and A. Massa, "Rectangular thinned arrays based on McFarland difference sets," *IEEE Trans. Antennas Propag.*, vol. 59, no. 5, pp. 1546-1552, May 2011.

[24] W. H. Weedon, W. J. Payne, and G. M. Rebeiz, "MEMS-switched reconfigurable antennas," in *Proc. Antennas and Propagation Society Int. Symp.*, vol. 3, Jul. 8-13, 2001, pp. 654-657.

[25] E. Fishler, A. Haimovich, R. Blum, D. Chizhik, L. Cimini, and R. Valenzuela, "MIMO radar: An idea whose time has come," in *Proc. IEEE Radar Conf.*, Apr. 2004, pp. 71-78.

[26] P. Stoica, J. Li, and Y. Xie, "On probing signal design for MIMO radar," *IEEE Trans. Signal Process.*, vol. 55, no. 8, pp. 4151-4161, Aug. 2007.

[27] S. Ahmed, J. S. Thompson, Y. R. Petillot, and B. Mulgrew, "Unconstrained synthesis of covariancematrix for MIMOradar transmit beampattern," *IEEE Trans. Signal Process.*, vol. 59, no. 8, pp. 3837-3849, Aug. 2011.

[28] G. Hua and S. S. Abeysekera, "MIMO radar transmit beampattern design with ripple and transition band control," *IEEE Trans. Signal Process.*, vol. 61, no. 11, pp. 2963-2974, Jun. 2013.

[29] H. L. Van Trees, *Detection, Estimation, and Modulation Theory, Part IV, Optimum Array Processing.* New York: Wiley, 2002.

[30] H. Cox, R. Zeskind, and M. Owen, "Robust Adaptive Beamforming," *IEEE Trans. Acoust. Speech Signal Process.*, vol. ASSP-35, no. 10, pp. 1365-1376, Oct. 1987.

[31] H. Cox, R. Zeskind, and T. Kooij, "Practical supergain," *IEEE Trans. Acoust. Speech Signal Process.*, vol. ASSP-34, no. 3, pp. 393-398, Jun. 1986.

[32] A. Antoniou, "Improved minimax optimization algorithms and their application in the design of recursive digital filters," *IEE Proc.*, vol. 138, no. 6, pp. 724-730, Dec. 1991.

[33] R. C. Nongpiur, D. J. Shpak and A. Antoniou, "Improved design method for nearly linear-phase IIR filters using constrained optimization," *IEEE Trans. Signal Process.*, vol. 61, no. 4, pp. 895-906, Feb. 2013.

[34] A. Antoniou, W.-S. Lu, *Practical Optimization: Algorithms And Engineering Applications*, Springer 2007.

[35] E. J. Candes, M. B. Wakin, and S. P. Boyd, "Enhancing sparsity by reweighted l_1 minimization," *J. Fourier Analy. Appl.*, vol. 14, pp. 877-905, Dec. 2008.

[36] W.-S. Lu and T. Hinamoto, "Optimal design of IIR digital filters with robust stability using conic-quadratic-programming updates," *IEEE Trans. Signal Process.*, vol. 51, no. 6, pp. 1581-1592, Jun. 2003.

[37] J. F. Sturm, "Using SeDuMi1.02, a MATLAB toolbox for optimization over symmetric cones," *Optim. Methods Softw.*, vol. 11ÂŰ12, pp. 625-653, 1999.

[38] R. C. Nongpiur and D. J. Shpak, "L-infinity norm design of linear-phase robust broadband beamformers using constrained optimization," *IEEE Trans. Signal Process.*, vol. 61, no. 23, pp. 6034-6046, Dec. 2013.

[39] H. L. Van Trees, "Optimum Array Processing, Part IV of Detection, Estimation and Modulation Theory," New York: Wiley, 2002.

[40] T. Isernia, O. M. Bucci, and N. Fiorentino, "Shaped beam antenna synthesis problems: Feasibility criteria and new strategies," *J. Electromagn. Waves Applicat.*, vol. 12, pp. 103-138, 1998.

[41] [Online]. Available: https://googledrive.com/host/0B6zSDcu_8P_EUjFCUVlWSFF2X3c/addDocTsp2014_1.pdf

Rajeev C. Nongpiur (S'01, AM'05, M'12) received the B.Tech. degree in Electronics and Communications Engineering from the Indian Institute of Technology, Kharagpur, India, in 1998 and the Ph.D. degree from the University of Victoria, British Columbia, Canada, in 2005. From 1998 to 2000 he worked as a Systems engineer at Wipro Technologies, from 2004 to 2008 as a Research Scientist at QNX Software Systems, from 2008 to 2010 as Senior DSP Engineer with Unication Co., Ltd., Vancouver, Canada, and from 2010 to 2014 as a Research Associate in University of Victoria. He is currently serving as Algorithm Engineer at Google Inc., Palo Alto, USA. His research interests are in the areas of signal processing for digital communications, multimedia, and biomedical applications. He is the author of more than 15 patents in the area of acoustic signal processing.

Dr. Nongpiur is a member of the IEEE Circuits and Systems and Signal Processing Societies.

Dale J. Shpak (S'79, M'86, SM'09) received the B.Sc. (Elec. Eng.) from the University of Calgary, Canada in 1980. From 1980 to 1982, he worked as an engineer for the City of Calgary Electric System while earning his M.Eng. in Electronics. Between 1982 and 1987, he performed research on computer systems, microelectronics, and DSP algorithms and implementation. From 1987 to 1989, he earned his Ph.D. at the University of Victoria, Canada. Starting in 1988, he served as a Professor with the Department of Engineering at Royal Roads Military College and returned to industry when it closed in 1995.

Since 1989 he has held a faculty position at the University of Victoria in addition to his other professional activities. As an Adjunct Professor of Electrical and Computer Engineering, he receives ongoing NSERC funding for research programs with his graduate students.

He joined the Dept. of Computer Science at Camosun College in 1999. He has instructed over thirty different courses including object-oriented programming, computer networks, digital circuit design, digital filters, materials science, software engineering, and real-time and concurrent systems.

He held several positions in industry where he developed algorithms, software, circuits, networking systems, and embedded systems. Since 1984, he has served as a consultant and develops software and embedded systems for products including audio processing, wireless sensing and control, and remote sensing. He is a principal developer of award-winning products, including the Filter Design Toolbox for MATLAB^{TM}.

Dr. Shpak is a Senior Member of the IEEE and a Member of the Association of Professional Engineers of the Province of British Columbia. His principal research interests are in the areas of signal processing for communications and audio, design and implementation of embedded systems, and digital filter design.

He also develops free software for music education.